Molecular Sorting of Lipids by Bacteriorhodopsin in Dilauroylphosphatidylcholine/Distearoylphosphatidylcholine Lipid Bilayers

Fabrice Dumas,* Maria M. Sperotto,# Maria-Chantal Lebrun,* Jean-François Tocanne,* and Ole G. Mouritsen#
*Institut de Pharmacologie et Biologie Structurale du CNRS, F-31062 Toulouse Cedex, France, and #Department of Chemistry, Technical University of Denmark, DK-2800 Lyngby, Denmark

ABSTRACT A combined experimental and theoretical study is performed on binary dilauroylphosphatidylcholine/distearoylphosphatidylcholine (DLPC/DSPC) lipid bilayer membranes incorporating bacteriorhodopsin (BR). The system is designed to investigate the possibility that BR, via a hydrophobic matching principle related to the difference in lipid bilayer hydrophobic thickness and protein hydrophobic length, can perform molecular sorting of the lipids at the lipid-protein interface, leading to lipid specificity/selectivity that is controlled solely by physical factors. The study takes advantage of the strongly nonideal mixing behavior of the DLPC/DSPC mixture and the fact that the average lipid acyl-chain length is strongly dependent on temperature, particularly in the main phase transition region. The experiments are based on fluorescence energy transfer techniques using specifically designed lipid analogs that can probe the lipid-protein interface. The theoretical calculations exploit a microscopic molecular interaction model that embodies the hydrophobic matching as a key parameter. At low temperatures, in the gel-gel coexistence region, experimental and theoretical data consistently indicate that BR is associated with the short-chain lipid DLPC. At moderate temperatures, in the fluid-gel coexistence region, BR remains in the fluid phase, which is mainly composed of short-chain lipid DLPC, but is enriched at the interface between the fluid and gel domains. At high temperatures, in the fluid phase, BR stays in the mixed lipid phase, and the theoretical data suggest a preference of the protein for the long-chain DSPC molecules at the expense of the short-chain DLPC molecules. The combined results of the experiments and the calculations provide evidence that a molecular sorting principle is active because of hydrophobic matching and that BR exhibits physical lipid selectivity. The results are discussed in the general context of membrane organization and compartmentalization and in terms of nanometer-scale lipid-domain formation.

INTRODUCTION

Biological membranes are organized structures with static and dynamic order on all length scales, ranging from the molecular scale to the size of the cell (Bloom et al., 1991; Lipowsky and Sackmann, 1995; Mertz and Roux, 1996). Paradoxically, many of the forces and mechanisms responsible for this complex organization involve physical forces (Israelachvili, 1992) that are not particularly strong on the scale of thermal energy. The organization of the fluid-bilayer component of the cell membranes is a particularly elusive problem in this context, because the bilayer membrane, in its physiological state, is in most cases a pseudo-two-dimensional fluid imparted with disorder due to high lateral diffusion of its molecular constituents. At the same time it is highly structured and compartmentalized (Edidin, 1990). The emergence of order and structure out of lateral disorder (Mouritsen and Jørgensen, 1994), together with the energetics of the underlying self-organizational principles, poses some of the major current problems in the biophysics of membranes.

A particular question is related to the existence of lipid domains on the nanometer scale (1–100 nm) (Bergelson et al., 1995) and the relationship between lipid-domain formation and the functional properties of membrane-associated proteins: both integral membrane proteins, such as bacteriorhodopsin (BR) (Rehorek et al., 1985; Piknová et al., 1993; Schram et al., 1994) and rhodopsin (Kusumi and Hyde, 1982), and peripherally bound proteins, such as cytochrome *c* (Mustonen et al., 1987) and phospholipase A_2 (Muderhwa and Brockman, 1992; Mouritsen and Biltonen, 1993; Lehtonen and Kinnunen, 1995; Hønger et al., 1996). In the case of integral membrane proteins, numerous attempts have been made experimentally as well as theoretically to investigate whether lipid-protein interactions can lead to a particular structuring of the exogeneous, nonchemically bound lipids around the proteins, i.e., whether proteins and enzymes display some kind of physical specificy or selectivity with respect to the lipids (Devaux and Seigneuret, 1985; Sperotto and Mouritsen, 1993; Tocanne et al., 1994). Both the lipid order parameter profile as well as the compositional profile around the protein are of interest in this context. Because the lipid bilayer membrane can be in a fluid phase, the lipid domains under consideration and the possible structuring of the lipidic environment of integral proteins are necessarily of a dynamic nature, i.e., described by a finite time scale and a length scale that at best can be characterized by a coherence or correlation range over which the particular structure can be discerned (Sperotto and Mouritsen, 1993). Lipid domains and annuli on the nanometer scale are therefore fluctuating entities subject to a rapid exchange of lipid molecules, and

Received for publication 2 December 1996 and in final form 19 March 1997.

Address reprint requests to Dr. Ole G. Mouritsen, Department of Chemistry, Technical University of Denmark, Building 206, DK-2800 Lyngby, Denmark. Tel.: +45-45-252462; Fax: +45-45-934808; E-mail: ogm@kemi.dtu.dk.

0006-3495/97/10/1940/14 $2.00

they are therefore difficult to detect experimentally. In contrast, lipid domains on the micron scale readily lend themselves to study by fluorescence microscopy (Grainger et al., 1989; Glaser, 1992; Tocanne, 1992).

Formation of dynamic lipid domains in the nanometer range is a mere consequence of the many-particle nature of the system, which endows the membrane with cooperativity and collective behavior. Some of the more spectacular consequences of this behavior are phase transitions and phase separation phenomena. In the case of equilibrium, phase separation leads to the formation of macroscopically large domains (phases), whereas out of equilibrium, the phase separation process may produce small-scale domains (Sankaram et al., 1992; Jørgensen and Mouritsen, 1995; Jørgensen et al., 1996). Within the equilibrium phases, dynamic lipid domains may arise because of density or compositional fluctuations (Mouritsen and Jørgensen, 1994). Therefore, the fluctuations are stronger and the domains larger as the system approaches phase boundaries and critical points. Domain formation due to density fluctuations can be visualized as regions of space where the lipid-acyl chains have a certain degree of conformational order, and hence the bilayer an effective thickness, that is different from its average value. In the case of compositional fluctuations (e.g., in a binary lipid mixture; Jørgensen et al., 1993) the domains have a local composition that is different from the global composition in the phase under consideration. The formation of lipid domains due to thermodynamic fluctuations can be described as lateral dynamic membrane heterogeneity (Mouritsen and Jørgensen, 1994). Some indirect experimental evidence is available that supports the existence of this type of heterogeneity in simple one- and two-component lipid bilayers (Pedersen et al., 1996; Lehtonen et al., 1996).

When integral membrane proteins are incorporated into lipid membranes, which are subject to this kind of lipid-domain formation, two effects will result (Mouritsen and Sperotto, 1992). On the one hand, the domain formation will be modulated by the presence of the protein in a way that reflects the lipid-protein interactions. On the other hand, the domain structure will influence the tension on the protein, which in some cases may introduce conformational changes in the protein and therefore couple indirectly to the protein function, as has recently been found in the case of the meta-I to meta-II transition in rhodopsin (Brown, 1994).

Turning now to the molecular mechanisms involved in the lipid-protein interactions, hydrophobic matching of lipid-bilayer thickness (i.e., lipid acyl-chain length) and hydrophobic thickness of integral membrane proteins has been proposed as an important determinator of the coupling between lipid structure and integral membrane proteins (Sackmann, 1984; Mouritsen and Bloom, 1984, 1993; Mouritsen and Sperotto, 1992). The hydrophobic matching principle has proved to be a useful concept in the study of a series of reconstituted lipid-protein systems, including BR (Piknová et al., 1993), rhodopsin (Brown, 1994; Kusumi and Hyde, 1982), cytochrome *c* oxidase (Montecucco et al., 1982), (Na^+-K^+)-ATPase (Johannsson et al., 1981b), Ca^{2+}-ATPase (Caffrey and Feigenson, 1981; Cornea and Thomas, 1994; Johannsson et al., 1981a), and photosynthetic reaction center and antenna proteins (Peschke et al., 1987).

In the case of a binary lipid system consisting of two lipid species with different hydrophobic chain lengths, the hydrophobic matching principle has been proposed to act as a mechanism for lipid sorting at the lipid-protein interface because the protein will, on a statistical basis, prefer to be associated with the lipid species that is hydrophobically best matched (Sperotto and Mouritsen, 1993) (cf. Fig. 1). This proposition was based on a theoretical model calculation, and it showed that the compositional profile that arises around the protein because of a coupling of the hydrophobic matching to the compositional fluctuations persisting in a binary mixture can be fairly long range and lead to an effective lipid specificity or selectivity of the protein without any chemical specificity being operative.

In the present paper we shall explore the possibility of molecular sorting of lipids by proteins, using a special model membrane that is particularly well suited to exploiting the effects of hydrophobic matching. The model system is a binary dilauroylphosphatidylcholine/distearoylphosphatidylcholine (DLPC/DSPC) lipid mixture reconstituted with BR. The two lipid species have very different hydrophobic chain lengths, which furthermore are each subjected to substantial changes with temperature because of their gel-to-fluid phase transition. Depending on their physical state, these lipids can match or mismatch the hydrophobic length of the protein (Piknová et al., 1993). The large difference in hydrophobic length of the two lipid species implies a strongly nonideal mixing behavior and phase equilibria that involve large regions of gel-fluid and gel-gel phase coexistence (cf. the phase diagram in Fig. 2) in which the two species are strongly segregated. Depending on the global phase of the mixture as well as of the local structure in terms of lipid domains, one would expect BR, via its specific hydrophobic length, to display a preference for one or the other lipid species. The challenge is then to design an

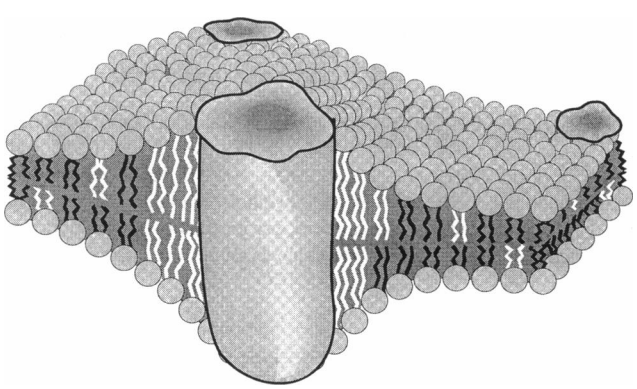

FIGURE 1 Skematic illustration of a lipid bilayer with embedded proteins and two different lipid species. The hydrophobic matching principle implies that there is an accumulation at the lipid-protein interface of the lipid species that is hydrophobically best matched to the protein.

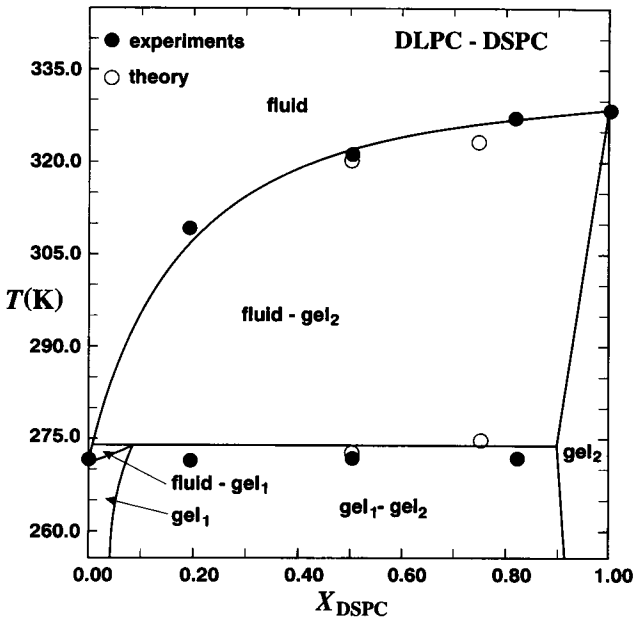

FIGURE 2 Temperature-composition phase diagram for DLPC/DSPC lipid mixtures. Data were obtained by differential scanning calorimetry (●) (Mabrey and Sturtevant, 1976). The open circles indicate the position of peaks of the calculated specific heat curves for two DLPC/DSPC mixtures (50%/50%) and (25%/75%). The solid lines are guides for the eye.

experiment that can investigate the possible consequences of such a specificity. We shall report here on an experimental approach that is built on the use of specifically designed fluorescent probes and provides evidence in favor of lipid sorting. The experimental work is supplemented by a theoretical calculation based on computer simulation of a specific microscopic molecular interaction model of the BR/DLPC/DSPC system. The model simulations have been inspired by the recent experimental work on the effect of bacteriorhodopsin on one-component lipid bilayers of different thicknesses (Piknová et al., 1993).

MATERIALS AND METHODS

Materials and preparation techniques

Chemicals

N-NBD-dilauroylphosphatidylethanolamine (N-NBD-C12-PE), N-NBD-egg-PE, egg yolk phosphatidylcholine (egg PC), DLPC, and DSPC were purchased from Sigma (St. Louis, MO). N-NBD-distearoylphosphatidylethanolamine (N-NBD-C18-PE) was synthesized as described by Monti et al. (1978). Then the fluorescent probe was purified by preparative silica gel thin-layer chromatography up to homogeneity. The elution solvent was $CHCl_3$/MeOH/CH_3COCH_3/CH_3COOH/H_2O (8:1:3:0.7:0.2, vol/vol).

Preparation of purple membrane and apomembrane

Purple membrane fragments were isolated from *Halobacterium halobium* according to well-established procedures (Oesterhelt and Stoeckenius, 1974). Partial delipidation was achieved by incubation of the membrane preparations in the presence of 3-[(3-cholamidopropyl)dimethylammonio]-1-propane-sulfonate 1% (w/v). After 48 h of contact, the detergent was removed by adsorption on hydrophobic resins (SM2 Biobeads), and membrane fragments were washed twice by centrifugation and resuspended in acetate buffer (100 mM Na-acetate, 150 mM NaCl, pH 5.0). Through determination of the protein (Peterson, 1977) and phosphorus (Eaton and Dennis, 1976) content, the purple membranes prepared in this way were found to contain approximately three polar lipid molecules per BR molecule.

Apomembranes were prepared by illumination of purple membrane samples (2×10^{-5} M) with a halogen lamp (KL 1500 electronic; Schott) in the presence of 200 mM hydroxylamine. After the purple color had completely disappeared, apomembrane fragments containing the bacterioopsin were collected by centrifugation, washed twice with the above acetate buffer, and subsequently used for reconstitution experiments.

Reconstitution of bacteriorhodopsin and bacterioopsin in lipid vesicles

The reconstitution procedure was essentially that described by Rigaud et al. (1995), which we have already used successfully (Piknová et al., 1993). Delipidated membranes (12 nmol protein), suspended in 1 ml of the acetate buffer, were mixed with 1 ml of an ether solution of N-NBD-phosphatidylethanolamine (N-NBD-PE) (12 nmol), N-NBD-C12-PE (12 nmol), or N-NBD-C18-PE (12 nmol) and the desired amount of phosphatidylcholines. The resulting two-phase system was sonicated at 4°C (25 pulses of 0.5 s each) with a B15 Branson sonifier (20 W, 40 kHz, 50% pulsed mode). The organic solvent was removed under reduced pressure (280–300 mm Hg) with a rotatory evaporator at a temperature 5°C above the gel-fluid phase transition temperature of the lipids used. When most of the organic solvent was removed, 1 ml of acetate buffer was added and evaporation was allowed to proceed for a further 20 min to remove all traces of solvent. Solvent evaporation usually took 20 min. For each reconstitution experiment, care was taken to recover the purple color, which was the first indication that reconstitution had occured without protein denaturation. Each sample was kept overnight at 4°C for equilibration. Bacteriorhodopsin concentration and absence of protein denaturation were assayed via the absorption spectrum of retinal. Absorption spectra of proteoliposomes were recorded with a Lambda 5 ultraviolet-visible spectrometer from Perkin-Elmer. Calculations were performed assuming an extinction coefficient of 63,000 M^{-1} cm^{-1} at 570 nm for retinal (Rehorek and Heyn, 1979) and a molecular mass of 26,400 Da for BR (Rehorek and Heyn, 1979). Any sample for which the spectrum of retinal was not correct in shape (position of the maximum absorption wavelength) and intensity (because of the amount and dilution state of the purple membrane used) was discarded. The ratio A_{570}/A_{280} was measured before and after every reconstitution experiment to ensure that it remained unchanged. As another control experiment, one aliquot (1 ml) of each proteoliposome sample was checked for homogeneity and composition. Reconstituted vesicles were centrifuged on a linear sucrose gradient (5–40%) with a Beckman L5-65 ultracentrifuge (100,000 × *g*, 4 h, 4°C). In most cases, a single and very sharp band was observed. Ten fractions of 1 ml each were collected and analyzed for their protein content by means of a modified Lowry protocol (Peterson, 1977). Their phospholipid content was checked by measuring the fluorescence of the 7-nitrobenz-2-oxa-1,3-diazol-4-yl (NBD) fluorophore. More than 90% of the reconstituted vesicles prepared by this procedure were found to be composed mainly (~95%) of proteoliposomes of uniform density (in fact, the sharp band corresponded to a volume of less than 0.1 ml) with the expected BR/DLPC/DSPC composition. In these preparations, nonreconstituted protein was absent, and the nonproteoliposome material (~5%) corresponded to BR-free lipid vesicles. The samples (less than 10%) that did not meet these criteria of homogeneity and composition were discarded. The gel-fluid phase equilibria of the lipid mixtures were monitored by fluorescence depolarization experiments using 1,6-diphenyl-1,3,5-hexatriene (DPH) as the probe. The phase diagram obtained by this approach was similar to that previously reported by Mabrey and Sturtevant (1976), who used differential scanning calorimetry techniques (cf. Fig. 2).

Fluorescence techniques

Fluorescence spectroscopy

Fluorescence emission spectra of proteoliposomes were recorded at various temperatures with a 500 SLM-Aminco spectrofluorimeter equipped with a thermostatted cuvette holder. Wavelengths of 465 nm and 535 nm were used for fluorescence excitation and emission, respectively. In the wavelength range of interest (350–600 nm), absorbance of proteoliposome dispersions was less than 0.1, enabling light scattering and inner filter effects to be ignored.

Fluorescence polarization

Experiments were carried out with an apparatus of our own fabrication, which has been described elsewhere (Piknová et al., 1993). The polarization p was expressed as

$$p = (I_V - I_H)/(I_V + I_H) \quad (1)$$

Theoretical model and computational techniques

Model

The theoretical model used in the present paper is a modification of a microscopic model (Sperotto and Mouritsen, 1993; Mouritsen et al., 1995) recently used to describe a two-component lipid bilayer incorporated with an immobile and very large protein, i.e., a protein whose cross-sectional diameter is much larger than the cross-sectional diameter of a lipid-acyl chain. Within this model the two lipid species are assumed to interact in a way that reflects the incompatibility of acyl chains of different hydrophobic lengths (Jørgensen et al., 1993). The extended model is then devised to include a finite concentration of large mobile proteins.

The model is built on the 10-state Pink model (Pink et al., 1980) to describe the gel-fluid transition for each of the pure lipid components in the fully hydrated state. The Pink model, which accurately accounts for the most important conformational states of the lipid chains and their mutual interactions and statistics, has proved useful for describing a wealth of thermodynamic, thermomechanic, and spectroscopic data for a variety of phospholipid membranes (Mouritsen, 1990; Mouritsen et al., 1995). Within the Pink model, the bilayer is considered as two independent monolayers, each represented by a triangular lattice on which the lipid chains are arrayed, one chain at each site. Each lipid acyl chain can take on one of 10 conformational states, each of which is characterized by a hydrocarbon chain length. Within the lattice formulation, a protein molecule can occupy a certain number of sites, n_P, and its hydrophobic part is assumed to be smooth and rodlike, and is characterized only by a cross-sectional area, A_P, and a length, d_P, of the hydrophobic protein domain.

The lipid-protein interactions have been incorporated into the microscopic Pink model in the form of attractive van der Waals-like interactions, and part of the interaction parameters have been identified in terms of a hydrophobic matching between the hydrophobic length of the lipid and that of the protein, in the spirit of the phenomenological mattress model of lipid-protein interactions in membranes (Mouritsen and Bloom, 1984, 1993). The interaction between lipids of the two different species is formulated in terms of an attractive van der Waals-like interaction and a repulsive mismatch interaction that reflects the possible incompatibility between chains with two different lengths. Details of the formalism used and the determination of the various parameters of the microscopic model can be found in the literature (Sperotto and Mouritsen, 1991a,b; Jørgensen et al., 1993). It should be pointed out that the interactions between the lipids and the proteins in this model are formulated in terms of physical forces, which implies that any association or selectivity that this model may predict is determined and controlled solely by these physical interactions.

The phase equilibria for the DLPC/DSPC mixture determined by Monte Carlo simulations on the microscopic model is shown in Fig. 2, together with the experimental phase diagram obtained by Mabrey and Sturtevant (1976) with differential scanning calorimetry. The theoretical phase boundaries were derived from peaks in the specific heat, $C_p(T)$, determined as a function of temperature for two different compositions.

The values of the lipid-protein interaction parameters of the model have been chosen to qualitatively reproduce the phase behavior of the dimyristoylphosphatidylcholine/bacteriorhodopsin (DMPC/BR) mixture (Piknová et al., 1993; Sternberg et al., 1989). The values of d_P and A_P characterizing BR have been chosen to model a protein size corresponding to that of BR (Henderson and Unwin, 1975), i.e., $d_P = 3$ nm and $A_P = 7$ nm^2.

Computational techniques

The microscopic and thermodynamic properties of the model have been calculated by standard Metropolis Monte Carlo simulation techniques (Mouritsen, 1990), in both the absence and presence of proteins. The thermal equilibrium is achieved by a combination of Glauber and Kawasaki dynamics. Glauber dynamics were used for the single-chain conformational excitations, and Kawasaki dynamics were used for the diffusive exchange of nearest-neighbor lipid chains as well as the diffusive exchange of protein molecules. The elementary movement of the protein molecules is assumed to correspond to translation of one lattice spacing in one of the six possible directions on the triangular lattice of lipid chains. The five lipid chains that have to be displaced by such a move are relocated from the front of the protein to the back of it in one single step.

The bulk thermodynamic state of the mixtures in equilibrium is characterized by calculating the specific heat per lipid molecule, $C_p(T)$, together with the average acyl-chain order parameter,

$$S = \left\langle \sum_{i=2}^{n} (3\cos^2\theta_i - 1)/[2(n-1)] \right\rangle \quad (2)$$

where the summation is over all n CH_2 segments of the acyl chain, and θ_i is the angle between the bilayer normal and the normal to the plane spanned by the ith CH_2 group of the chain.

To characterize the lateral structure and the coherence of short-range ordering phenomena, we have calculated the lipid concentration profiles, $F(L)$, as a function of the distance, L, from each protein surface (i.e., at the interface with the lipids), where L indexes the lattice site layers around each protein. In each layer L, $F(L)$ denotes the number of lipid molecules of a particular species normalized to the total number of molecules present in that layer.

Most of the simulations are performed on a triangular lattice of 40×40 sites, although a 60×60 lattice size has also been considered in a few cases. To simulate bacteriorhodopsin, each protein molecule is taken to occupy $n_P = 19$ lattice sites.

RESULTS

Experimental results

Fluorescence energy transfer experiments

General considerations and behavior of bacteriorhodopsin in egg PC vesicles. Fluorescence energy transfer is a well-established procedure for measuring distances in biological systems. In the present work this technique was used to study the spatial relationship between NBD-labeled phospholipids as donors and the retinal group of bacteriorhodopsin as an acceptor. As can be seen in Fig. 3, there is a significant overlap between the emission band of the NBD fluorophore and the absorption band of retinal, such that these two chromophores constitute an efficient donor-acceptor pair for resonance energy transfer experiments. Two important parameters are to be considered: 1) r_c, the dis-

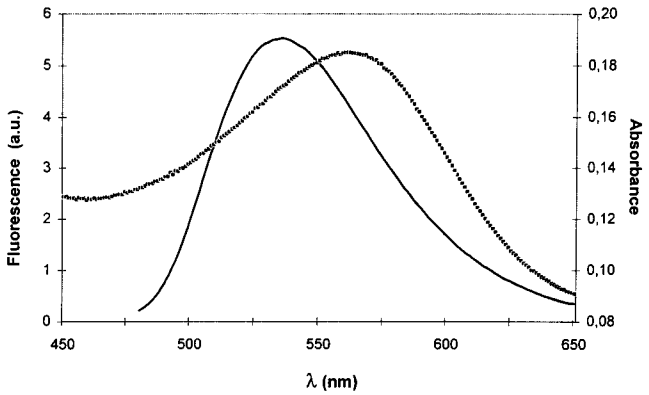

FIGURE 3 Fluorescence emission spectrum of the NBD-labeled probe (——) and the absorption spectrum (■) of retinal in bacteriorhodopsin in the form of water-suspended purple membrane fragments.

tance of closest approach of the two groups, and 2) R_0, the donor-acceptor distance for which the fluorescence energy transfer efficiency, E, is 50%. When attached to the polar headgroup of phosphatidylethanolamine, the NBD group has been shown to be located at the water/lipid interface in the polar headgroup region (Mazères et al., 1996). From x-ray crystallography data (Henderson et al., 1990), the retinal group can be assumed to be located near the center of bacteriorhodopsin, i.e., near the center of the lipid bilayer, along the symmetry axis of the protein. Assuming the protein to be of cylindrical shape with a circular cross section of 1.5 nm radius and a hydrophobic length of 3–3.1 nm (Henderson and Unwin, 1975; Piknová et al., 1993), and assigning molecular areas of 0.46 nm^2 (Kechuan et al., 1996) and 0.63 nm^2 (Nagle, 1993) to the lipids in the gel and fluid conformational states, respectively, lead to r_c values of 2.5 nm and 2.55 nm in the gel and fluid states, respectively. In the following, an r_c value of 2.5 nm was used. R_0 can be calculated using the following equations (Hasselbacher et al., 1984):

$$R_0 = (JK^2\Phi_D n^{-4})^{1/6}(9.7 \times 10^3) \quad (3)$$

with

$$J = \int F_D(\lambda)\varepsilon_A(\lambda)\lambda^4 d\lambda / \int F_D(\lambda)d\lambda \quad (4)$$

and

$$\Phi_D = \Phi_{ref}[n_D^2 A_{ref} F_D]/[n_{ref}^2 A_D F_{ref}] \quad (5)$$

where labels A and D designate the acceptor and donor molecules, respectively, and the subscript ref refers to a reference compound. Φ_D is the quantum yield of the donor in the absence of an acceptor, n is the refractive index, J is the spectral overlap integral, and K is the orientation factor. $F_D(\lambda)$ is the fluorescence intensity of the donor in the absence of an acceptor at wavelength λ, and $\epsilon_A(\lambda)$ is the molar absorption coefficient of the acceptor at wavelength λ (Werner and Hoffman, 1973). F_D is the area under the corrected emission spectrum, and A_D is the absorbance of the solution at the excitation wavelength.

From the emission spectrum of NBD-labeled lipids and the absorption spectrum of retinal, a value of 3.58×10^{-13} M^{-1} cm^3 was calculated for J by numerical integration. K^2 was assumed to be 2/3, which corresponds to the case of rapid relative motion (and axial symmetry of the system). The refractive index of water (n = 1.33) was used. Because the fluorescence emission of the NBD group depends on both temperature and environmental factors, the quantum yield of the NBD-labeled lipids was measured in egg PC bilayers over the temperature range 268–338 K. 7-Dimethylamino-3-(*p*-formylstyryl)-1,4-benzoxazine-2-one (Φ_{ref} = 0.58 in ethanol, n_{ref} = 1.36) (Le Bris et al., 1984) was used as the reference compound. Measured Φ_D values and corresponding calculated R_0 values showed a linear dependence on T (r = 0.99), with Φ_D = 0.35 and R_0 = 5.5 nm at 268 K and Φ_D = 0.08 and R_0 = 4.2 nm at 338 K (data not shown). With an r_c value of 2.5 nm, we were in the situation where $r_c < R_0$, which has been analyzed recently by Yguerabide (1994). A Stern-Volmer equation can still be used to account for changes in fluorescence intensity, but now in the form

$$I_0/I = 1 + \gamma K_q \sigma \quad (6)$$

where I_0 and I are, respectively, the fluorescence intensities in the absence and presence of an acceptor, K_q is the steady-state quenching constant, σ is the acceptor surface density (molecules/cm^2), and γ is a correction factor that depends on the value of r_c/R_0. K_q is in units of reciprocal density (cm^2/molecule) and is defined by

$$K_q = (\pi R_0^2/2)(R_0/r_c)^4 \quad (7)$$

The correction factor γ was calculated by Yguerabide (1994). However, this factor can also be evaluated experimentally by measuring the influence of σ on I_0/I at various temperatures. For this purpose, BR was reconstitued into egg PC vesicles in the presence of N-NBD-egg PE. The donor (NBD):acceptor (retinal) molar ratio was kept constant at 1:1 as increasing amounts of egg PC molecules were added, to decrease the protein surface density. σ was calculated, assuming a molecular area of 6.90 nm^2 for the protein in the monomeric form (Henderson et al., 1990) and a molecular area of 0.63 nm^2 for egg PC (Nagle, 1993). The data obtained at a temperature of 293 K are shown in Fig. 4. As expected, I_0/I increased with increasing σ. As a control experiment, fluorescence intensities from lipid vesicles containing the donor only and from vesicles containing the donor and bleached bacteriorhodopsin were compared. They were identical, indicating that the fluorescence quenching observed in the presence of bacteriorhodopsin was due to a resonance energy transfer mechanism and not to self-quenching of the probes. The data in Fig. 4 can be accounted for by a straight line (r = 0.85). From the slope of this line and from Eqs. 6 and 7 one can calculate γ to be 0.145. Fluorescence energy transfer experiments carried out

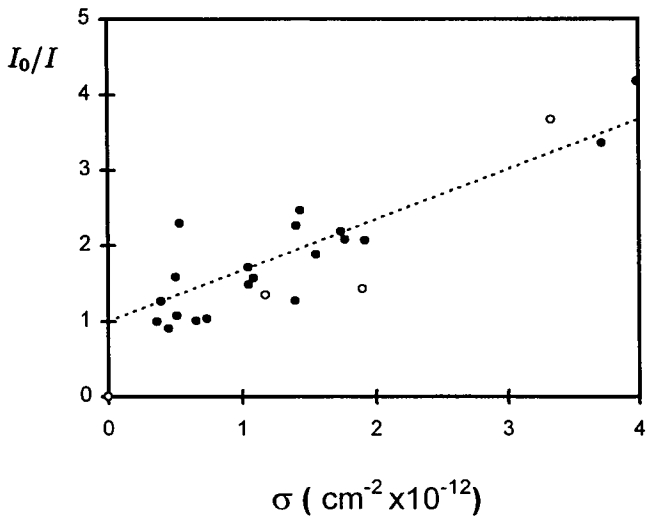

FIGURE 4 Influence of bacteriorhodopsin surface density σ (molecules/cm^2) on fluorescence energy transfer I_0/I. The host lipids are egg-PC with the probe N-NBD-PE (●) and DSPC with the probe N-NBD-C18-PE (○). The temperature is 293 K.

at 268 K and 338 K yielded γ values of 0.1 and 0.298, respectively. As can be seen in Fig. 5, these experimental γ values and corresponding r_c/R_0 ratios compare very well with the plot of γ versus r_c/R_0 determined by Yguerabide (1994).

The fluorescence quantum yield of NBD-labeled lipids is known to depend on the physical state (gel or fluid) of the lipids (Mazères et al., 1996), and one could argue that the above results are valid for lipids in the fluid phase only. Although the ratio I_0/I is expected to compensate for possible changes in fluorescence quantum yield, further control experiments were carried out, consisting of measuring fluorescence energy transfer between BR and the probe N-NBD-C18-PE in DSPC at 293 K, i.e., with lipids in the gel state. Three protein/lipid ratios were tested, and as can be seen in Fig. 4, the corresponding I_0/I values were similar to those obtained with egg PC for the same protein/lipid ratios.

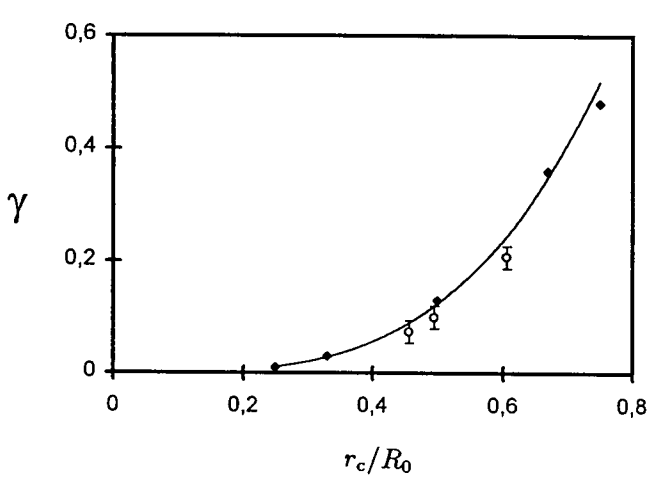

FIGURE 5 Plot of the correction factor γ in Eq. 9 versus r_c/R_0. ◆, Data reproduced from Yguerabide (1994); ○, results from the present work.

In conclusion, the approach described above can be used safely for interpreting the efficiency of fluorescence energy transfer in terms of acceptor surface density and consequently in terms of distribution of a given type of lipid probe and host lipid around the protein, whatever the phase state of the lipids.

Behavior of bacteriorhodopsin in DLPC/DSPC vesicles. Distribution of bacteriorhodopsin in DLPC/DSPC mixtures was studied with either N-NBD-C12-PE or N-NBD-C18-PE. As previously shown (Mazères et al., 1996), the NBD group in N-NBD-PE molecules stays at the water/lipid interface and has no influence on the lipid molecular packing. The phase behavior of these molecules depends on their acyl chains, and under the present conditions, the two probes can be used to monitor the behavior of the protein with respect to either the short-chain (DLPC) or the long-chain (DSPC) lipid molecules.

A protein/lipid molar ratio of 1/590 was used, with 25 mol% DLPC (147 molecules) and 75 mol% DSPC (443 molecules). This lipid composition was selected for the following three reasons:

1. By the hypothesis that BR and N-NBD-C12-PC are exclusively associated with DLPC molecules, the resulting and relatively high BR/DLPC and probe/DLPC molar ratio of 1/147 would still be low enough to ensure the existence of the protein in the monomeric state on the one hand (Piknová et al., 1993) and an absence of probe self-quenching on the other.

2. Depending on whether the protein and probe molecules are exclusively associated with DLPC or distribute within all of the lipids, the changes in protein surface density that would result are large enough to affect fluorescence energy transfer significantly.

3. The three polar lipids that remained associated with each protein molecule represent only 0.5 mol% of the exogenous lipids. They have been shown not to affect the phase behavior of DLPC and DSPC up to a concentration of 2 mol% (Piknová et al., 1993). Fluorescence energy transfer experiments were carried out over the temperature range of 268–338 K. As can be seen in Fig. 6 *a*, fluorescence energy transfer efficiency of the probe N-NBD-C12-PE remains practically unchanged at a relatively high value of ~60% up to a temperature of 306 K, above which it drops rapidly to less than 20% for temperatures above 325 K. An opposite although less pronounced effect was observed with the probe N-NBD-C18-PE, with a rather low fluorescence quenching of ~5% at 268 K, which increased progressively to ~20% at 298 K, above which it remained unchanged.

For each temperature tested, the ratio $(I_0-I)/I_0$ can be expressed in terms of an apparent protein surface density, σ, by means of Eqs. 6 and 7 and using the correponding calculated R_0 value together with the γ value interpolated from the data in Fig. 5. As can be seen in Fig. 6 *b* for the probe N-NBD-C12-PE, σ remained essentially unchanged

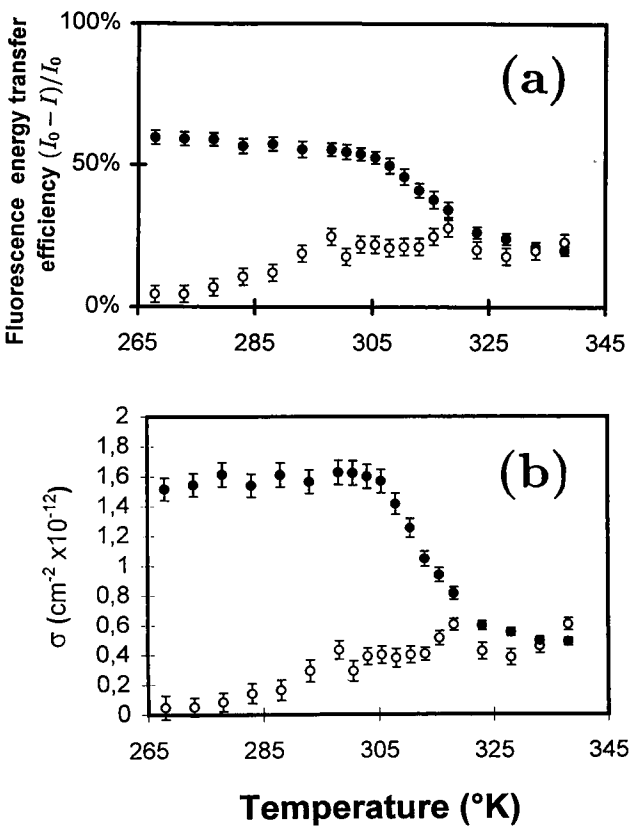

FIGURE 6 Temperature dependence of (*a*) the fluorescence energy transfer efficiency, $E = 1 - I/I_0$, and (*b*) the apparent protein surface density, σ, for bacteriorhodopsin reconstituted in DLPC/DSPC vesicles, in the presence of N-NBD-C12-PE (●) or N-NBD-C18-PE (○). The experiments with N-NBD-C12-PE were carried out in quadriplicate. Vertical bars indicate the dispersion of the data.

at the relatively high value of 1.6×10^{12} molecules/cm^2 up to the temperature of 306 K. Then it rapidly decreased to a low of 0.5×10^{12} molecules/cm^2 for temperatures above 325 K. For the probe N-NBD-C18-PE, σ progressively increased from a low of 0.05×10^{12} molecules/cm^2 at 268 K to 0.6×10^{12} molecules/cm^2 at 338 K. In fact, it should be remembered that in these experiments, the overall protein-to-lipid ratio was fixed at one protein to 590 lipids, which would correspond to an overall protein surface density of 0.52×10^{12} molecules/cm^2 if all of the lipids are in the fluid state (lipid molecular area $A_L = 0.63$ nm^2) or 0.7×10^{12} molecules/cm^2 if all of the lipids are in the gel state ($A_L = 0.46$ nm^2).

Fluorescence polarization experiments

Because of the large difference in hydrophobic length, DLPC and DSPC exhibit strong nonideal mixing, implying large regions in the phase diagram (cf. Fig. 2), where pronounced gel-fluid and gel-gel phase coexistence regions arise. The large differences observed above between the experimental and predicted apparent protein surface densities and their dependence on temperature and the lipid probe used, strongly suggest that in DLPC/DSPC mixtures, the distribution of BR is not random, but depends on the lateral distribution of lipids in connection with their physical state. From the phase diagram in Fig. 2 it can be inferred that for the 25/75 molar ratio, the lipids are in the gel state below 271 K, which corresponds to the beginning of the melting of a nearly pure DLPC phase, and in the fluid state above 326 K, which corresponds to the end of the melting of a DSPC-rich phase. To determine the temperature at which the DLPC-rich phase completed melting and the DSPC-rich phase started to melt in the absence and in the presence of BR, DLPC/DSPC liposomes ($X = 0$) and BR/DLPC/DSPC reconstitutions ($X = 1/590$) were submitted to fluorescence polarization experiments, with DPH as a probe. The results are displayed in Fig. 7, which shows that for both systems, very similar triphasic polarization curves were obtained as a function of temperature, clearly indicating in both cases a melting of a DLPC-rich phase up to a temperature around 280 K and a melting of a DSPC-rich phase between 310 K and 325 K. This demonstrates that the protein in this concentration showed little influence on the phase equilibria of the binary lipid mixture. Furthermore, the melting of the DSPC-rich phase occurred over the same temperature range that is associated with a large decrease in the fluorescence quenching of the probe N-NBD-C12-PE. This result indicates that in BR/DLPC/DSPC reconstitutions, the apparent surface density measured for BR with the short-chain or the long-chain probe is to be correlated with the physical state of the host lipids and their distribution within the various coexisting phases.

Theoretical results

Binary mixture: DLPC/DSPC

We shall briefly describe the computer simulation results shown in Figs. 8 and 9 obtained for the binary lipid mixture in the absence of the protein, to provide a basis for clarifying the influence of the protein on the bilayer thermodynamics and molecular order.

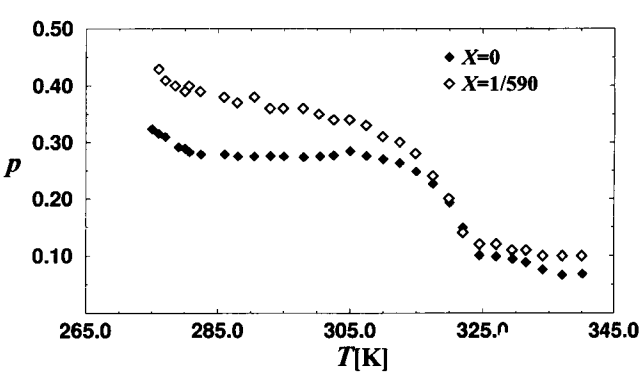

FIGURE 7 Influence of temperature on the polarization of DPH inserted in the binary mixture DLPC/DSPC (25%/75%) with no BR (◆, $X = 0$) and in the BR/DLPC/DSPC (1:147:443) reconstitutions (◇, $X = 1/590$).

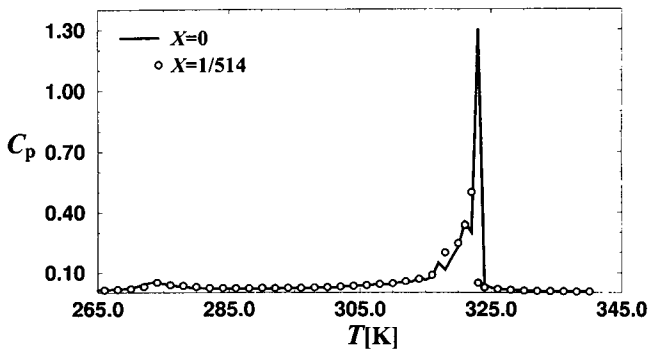

FIGURE 8 Calculated specific heat curves $C_p(T)$ for DLPC/DSPC mixtures (25%/75%) with BR-to-lipid ratios: $X = 0$ (——) and $X = 1/514$ (○). $C_p(T)$ is given per lipid molecule in units of 10^{-13} erg K^{-1}.

The specific heat shown in Fig. 8 displays two peaks indicating the position of the phase boundaries. Because of the stong demixing in this system, the two peaks represent to a good approximation the individual melting of the two species. The peak associated with the melting of DLPC is broader and weaker than that of DSPC at this composition, in good accordance with the experimental data obtained from the fluorescence polarization shown in Fig. 7 and data from differential scanning calorimetry (Mabrey and Sturtevant, 1976). This is due to the fact that the melting transition of the short-chain phospholipid is much more strongly influenced by density fluctuations (Ipsen et al., 1990).

The more pronounced and localized melting behavior of the long-chain lipid is reflected in the behavior of the acyl-chain order parameters shown in Fig. 9, which also parallels that of the fluorescence polarization shown in Fig. 7. A similar thermal asymmetry in the order parameters due to the nonideal mixing of short- and long-chain phospholipids has also been observed for DMPC/DSPC mixtures (Sankaram et al., 1992; Brumm et al., 1996).

Ternary mixture: BR/DLPC/DSPC

The results discussed below refer to the experimental lipid composition of 25%/75% mole concentration of DLPC/DSPC phospholipid mixtures and to a BR-to-lipid molar ratio $X = 1/514$. Within the lattice formulation used for the modeling and for a protein that occupies $n_P = 19$ lattice sites, the choice of $X = 1/514$ is the closest possible to the experimental ratio 1/590 in the case of a lattice with 40×40 sites. For lattice sizes of 60×60, the corresponding closest molar ratio is $X = 1/581$.

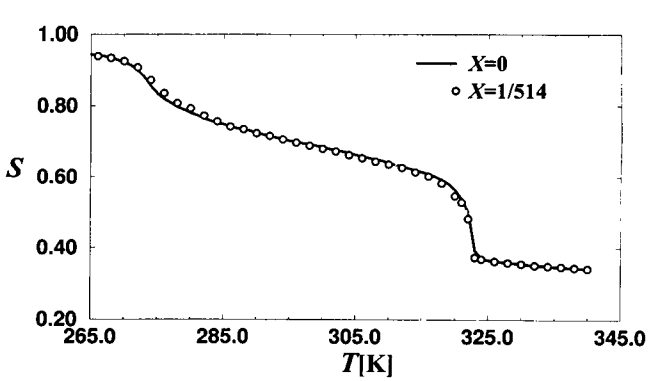

FIGURE 9 Calculated average acyl-chain order parameter S in Eq. 2 versus T for DLPC/DSPC mixtures (25%/75%) with BR-to-lipid ratios $X = 0$ (——) and $X = 1/514$ (○).

The simulation data are presented in Figs. 8–11. The presence of the protein in these low concentrations is seen to only insignificantly influence the bulk properties of the binary lipid mixture, i.e., the specific heat and the acyl-chain order parameters are basically unchanged. This is in accordance with the fluorescence polarization results reported above.

Whereas the bulk properties of the ternary mixture are unaffected by the presence of the protein, there is a distinct local demixing of the lipid mixture taking place near the protein, as seen in the lipid concentration profiles, F, in Fig. 10. This is particularly clear for $T = 310$ and 338 K. Note that the profiles at the lower temperature, $T = 268$ K, reflect the massive gel-gel phase separation, and their form is influenced by the finite size of the system studied. This is also the case for the data in the gel-fluid coexistence region at large separations L. The lipid concentration profiles show that near the protein surface there is an enrichment of one of the species and a depletion of the other one in a systematic fashion, reflecting the hydrophobic matching. Melted-state DSPC is selected by the protein in the fluid phase and the fluid-gel coexistence region because of the better hydrophobic match. This is also clear from the microconfigurations shown in Fig. 10. The lipids are selected on a statistical basis, and their lateral distribution close to the protein is not static but dynamic, because there is no specific binding of the lipid molecules to the protein. In the gel-gel coexistence region, the proteins are better matched by gel-state DLPC, and their environment is therefore enriched by DLPC, in fact, to such an extent that the proteins are found predominantly in the DLPC-rich gel phase. It is also observed from the microconfiguration at $T = 310$ K corresponding to the gel-fluid coexistence region that the proteins tend to be adsorbed at the phase boundaries with a region of fluid DSPC around them. This interfacial adsorption effect is generally expected in many-phase systems with "impurities" that have no particular preference for any particular phase and are therefore expelled to the boundary. In this case, both lipid phases imply a hydrophobic mismatch, and it is therefore unfavorable for the lipids to disperse the proteins.

Despite the local demixing of the lipids, BR is still, on average, dissolved in the DLPC-rich phase whenever this is available, in accordance with the fluorescence energy transfer data reported above, which clearly indicate a high apparent surface density for the protein up to a temperature of ~310 K before the melting of the DSPC-rich phase.

Because in the computer simulation calculations all molecular variables are available, it is possible to calculate several different observables that can be related to proper-

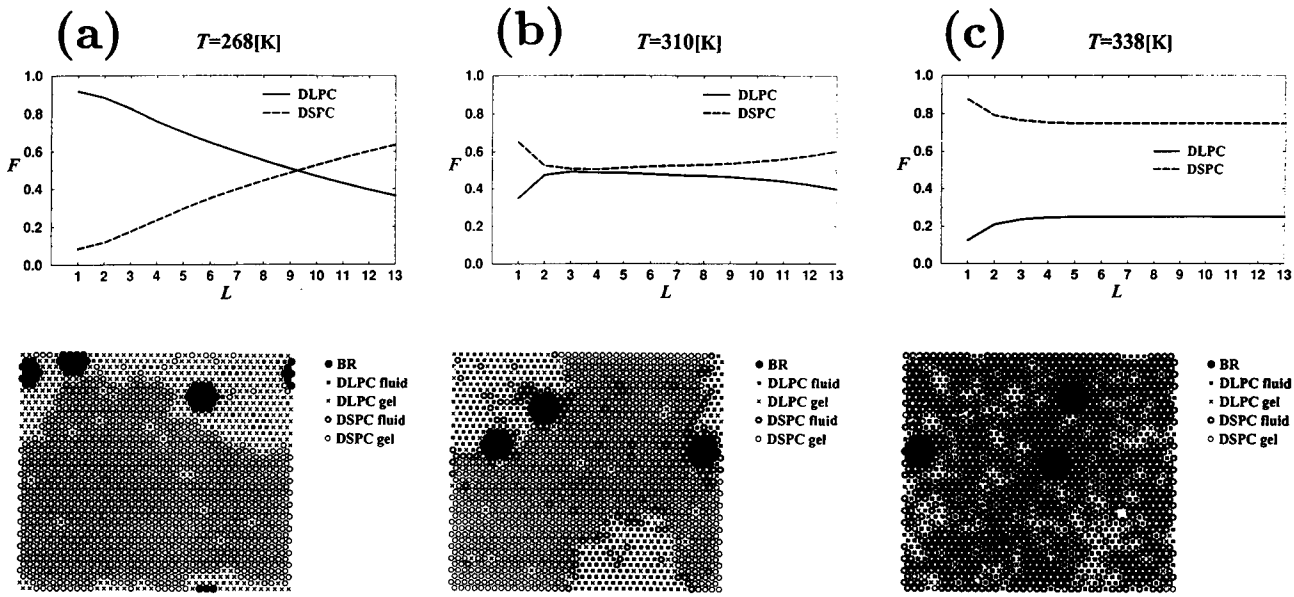

FIGURE 10 Lipid concentration profiles $F(L)$ versus layer index L around a BR molecule in a DLPC/DSPC (25%/75%) mixture, with a BR-to-lipid ratio of $X = 1/581$. The $F(L)$ data refer to simulations on a lattice size of 60×60 sites. The data refer to the following temperatures: $T = 268$K (a), $T = 310$K (b), and $T = 338$K (c). Below are shown typical microconfigurations corresponding to the same temperatures. The symbols indicate the following: black, BR; ×, DLPC; ○, DSPC; small symbols, gel; large symbols, fluid. The microconfigurations refer to simulations on a lattice with 40×40 sites and hence a protein concentration of $X = 1/514$.

ties derived from the experimental data. A particularly interesting and key parameter derived from the experimental data is the acceptor (protein) surface density, σ, and its dependence on temperature. To calculate σ from the simulation data, a number, N, of either DLPC or DSPC chains have been labeled as "donors." As in the experiments, this number is taken to be equal to the number of BR molecules. The BR surface density is then calculated by summing over all donors (labeled by i):

$$\sigma = \left\langle \sum_{i=1}^{N} N_{BR}(i)/(\pi \bar{R}^2 N) \right\rangle$$

where $N_{BR}(i)$ is the number of BR (acceptors) that are found to be present around donor i within a distance $\bar{R}$ from the donor. $\bar{R}$ is assumed to be equal to R_0, the donor-acceptor distance for which the fluorescence energy transfer is 50%. To derive σ from the simulations, the value of R_0 has to be put in. From the experiments, R_0 is known at two temperatures, $T = 268$ K and 338 K, i.e., in the gel-gel coexistence region and in the fluid phase. We have assumed that the value of R_0 is constant within each of these phases, and that its value in the gel-fluid coexistence region is the average of these two values. The results for σ as a function of temperature across the phase diagram are shown in Fig. 11, together with the values derived from the experimental data. In the case where the "donors" are the short-chain lipids, the simulation data and the experimental data within the gel-gel coexistence region and within the fluid phase are in good agreement, whereas within the gel-fluid coexistence region there is some deviation. The constant level of σ reached for temperatures above $T \simeq 325$ K corresponds to a random distribution of the molecules, whereas the increasing value of σ for lower temperatures indicates that BR molecules statistically prefer to be surrounded by DLPC molecules. In the case where the "donors" are the long-chain lipid, the values predicted for σ show a slight increase with temperature, reaching a constant level in the fluid phase. This indicates that at low temperatures, the BR molecules avoid contact with DSPC lipids. We return below to a comparison between the simulation and the experimental data for σ.

COMPARISON BETWEEN EXPERIMENTAL AND THEORETICAL RESULTS

From the phase diagram of DLPC/DSPC mixtures (Fig. 2) and fluorescence polarization data of bacteriorhodopsin re-

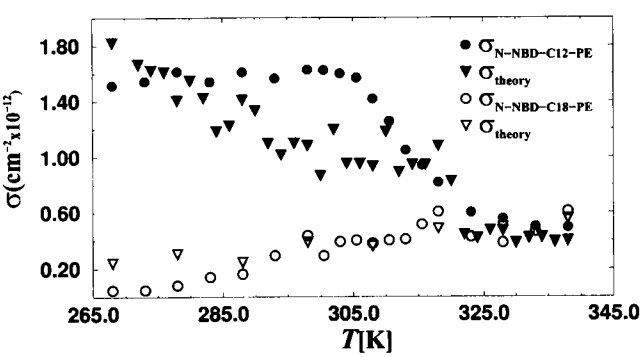

FIGURE 11 BR protein surface density, σ, versus temperature, obtained by calculations based on either the experimental data (●, ○; cf. Fig. 6, a and b) or the computer simulation data (▲, △; cf. Eq. 8).

constitutions (Fig. 7), as well as the computer simulation results, one can, to a good approximation, assume that at 268 K most of the lipids are in the gel state (gel-gel coexistence region), that at 293 K most of the DLPC lipids are in the fluid state whereas most of the DSPC lipids are still in the gel state (fluid-gel state), and that at 338 K all of the lipids are in the fluid state. Using a molecular area of 6.90 nm^2 for the protein and 0.46 nm^2 and 0.63 nm^2 for the lipids in the gel and fluid states, respectively, one can calculate that at 268 K, an apparent surface density of 1.51×10^{12} molecules/cm^2 with respect to the short-chain lipid probe is equivalent to one protein molecule associated on the average with 257 lipid molecules in the gel state, which distribute over 4.6 layers around the protein. This number of lipid molecules is too large compared to the 147 DLPC molecules available on the average and too low compared to the overall number of 590 lipid molecules associated on the average with one protein molecule. At 338 K, an apparent surface density of 0.49×10^{12} molecules/cm^2 corresponds to 623 lipid molecules in the fluid state distributing over 8.2 layers around one protein, a value that is slightly in excess compared to the 590 lipid molecules associated with one BR molecule, and which can distribute over 7.9 layers when in the fluid state. The large differences observed at low temperature between the apparent and real lipid distributions around the protein can easily be understood if one recalls that bacteriorhodopsin prefers DLPC in the gel state compared to DSPC and that extensive phase separation takes place between the two lipid species in this temperature range.

These comparisons between experimental and calculated lipid distributions can be considerably improved when taking into account the lipid distributions obtained from the computer calculations (cf. Fig. 10). Indeed, from the data in Fig. 4 obtained from a one-component system, it is possible to estimate in a recurrent way the contribution of the probe N-NBD-egg PE to the fluorescence energy transfer process when located in the first, second, third, and ith layer around the protein. In this calculation and in the following, the probability of finding the probe in a given layer is assumed to be proportional to the fractional number of lipid molecules in this layer. Then, for the two-component system DLPC/DSPC, the compositional profiles shown in Fig. 10, *a* ($T = 268$ K) and *c* ($T = 338$ K), are used to calculate the distribution of the probe N-NBD-C12-PE or the probe N-NBD-C18-PE in the various layers around the protein. Finally, from these distributions and the above-calculated contributions, one can estimate for each probe the I_0/I ratios and therefore the apparent protein surface density σ. As can be seen in Table 1 for the probe N-NBD-C12-PE, good agreement between experimental and predicted values is observed for lipids in both the gel and fluid phases, which provides a straightforward explanation for the actual lipid distribution around the protein. At 268 K in the gel phase, a protein surface density of 1.51×10^{12} (calculated 1.54×10^{12}) molecules/cm^2, which corresponds to 257 (calculated 252) lipid molecules and a value of $n_\ell = 4.6$ (calculated 4.5) lipid layers around each protein, does account for the existence of BR in a nearly pure DLPC phase. That this value is larger than that expected is due to the fact that the two species are not fully separated, but there is a small but finite solubility of DLPC molecules in the DSPC-rich domains far from the protein. At 338 K in the fluid phase, an apparent protein surface density of $\sigma = 0.49 \times 10^{12}$ molecules/cm^2 corresponds to 623 lipid molecules distributing over 8.2 lipid layers and accounts for the presence of the protein in a mixed lipid phase. Recalculation of the fluorescence energy transfer parameters as described above yields similar values, $\sigma = 0.47 \times 10^{12}$ molecules/cm^2, 650 lipid molecules and 8.4 lipid layers. The expected values for lipids in the fluid phase and in the case of a random distribution around the protein are 590 molecules and 7.9 layers, respectively.

With the probe N-NBD-C18-PE at low temperatures, the fluorescence energy transfer is too low (i.e., I_0/I close to unity) to be interpreted quantitatively. However, consistent with the above results, such a low ratio suggests an absence of the long-chain probe in proximity to the protein and therefore a marked preference by the protein for the short-chain lipids in the gel phase. In the gel-fluid phase coexistence region, between 275 K and 305 K, the progressive increase observed in fluorescence energy transfer and in σ with increasing temperature (cf. Fig. 6, *a* and *b*) may be explained by the fact that the melted DSPC molecules, which progressively enter the DLPC-rich phase, are selected by the protein because of the better hydrophobic match (cf. Fig. 10). For temperatures above 320 K, in the fluid phase, I_0/I assumes an average value of 1.28, to which corresponds a σ value of 0.55×10^{12} molecules/cm^2, equivalent to 555 lipid molecules distributed over 7.7 layers around the protein. These values also account for the presence of the protein in a fluid mixed lipid phase. They are consistent

TABLE 1 Experimental and calculated values for the fluorescence intensity ratio, I_0/I, the apparent protein surface density, σ (molecules/cm^2), and the corresponding number, n_ℓ, of lipid layers around the protein

	Experimental			Calculated		
Temp (K)	I_0/I	σ ($\times 10^{-12}$)	n_ℓ	I_0/I	σ ($\times 10^{-12}$)	n_ℓ
268	2.45 ± 0.3	1.51 ± 0.3	4.6 ± 0.6	2.5	1.54	4.5
338	1.25 ± 0.05	0.49 ± 0.01	8.2 ± 1.0	1.24	0.47	8.4

Note that the 590 lipid molecules associated with one bacteriorhodopsin molecule distribute over 7.7 and 7.9 layers around the protein when in the gel and fluid phase, respectively.

with recalculated values of $I_0/I = 1.27$, $\sigma = 0.53 \times 10^{12}$ molecules/cm^2, 576 lipid molecules, and $n_1 = 7.8$. To account quantitatively for these results in terms of lipid sorting by the protein may be difficult because, in the fluid phase, the fluorescence approach reaches its limits of resolution: 1) the fluorescence signal is lower in the fluid phase than in the gel phase because of a large decrease in the fluorescence quantum yield of the NBD group with increasing temperature (fourfold decrease from 268 K to 338 K); 2) the average distance between the donor and acceptor chromophores becomes large (corresponding to low I_0/I values); 3) only small deviations from a random distribution of DLPC and DSPC around the protein are expected. In the present study, the difference between the lipid distributions detected by the two probes lies within the experimental error, and despite qualitative agreement with recalculated distributions, one cannot definitely conclude that in the fluid phase bacteriorhodopsin prefers DSPC as compared to DLPC. Nevertheless, the good agreement between the experimental and theoretical data observed in the gel-gel and gel-fluid coexistence regions gives strong support to the theoretical prediction that, in the fluid phase, at least the first layer around bacteriorhodopsin is enriched in DSPC at the expense of DLPC.

We now turn to a comparison between the experimental and simulation data for the BR surface density, σ, shown in Fig. 11. Considering the approximations entering the derivation of σ from the simulation data, the accordance between the two sets of data in Fig. 11 is satisfactory. The systematic deviation in the gel-fluid coexistence region between the theoretical and experimental results for σ related to the N-NBD-C12-PE probe may indicate that the localization of BR in the boundaries between the gel and fluid domains may be statistically overestimated in the simulations or it may indicate that the experimental system is not fully phase separated. This last possibility should be seen in light of the very slow phase separation dynamics that is known to persist in binary mixtures of lipids with very different chain lengths (Jørgensen et al., 1996).

In general, the theoretical model simulations support the interpretation of the experimental data in terms of molecular sorting of lipids at the hydrophobic interface between BR and the lipid-bilayer matrix and how this sorting depends on the thermodynamic conditions (i.e., temperature and composition).

DISCUSSION AND CONCLUSIONS

We have in this paper presented a two-pronged approach to one of the more elusive problems in membrane biophysics related to the lipid selectivity of integral membrane proteins. Guided by a theoretical concept, the hydrophobic matching principle (Mouritsen and Bloom, 1993), we have carried out a parallel experimental and theoretical model study of a specific model membrane, BR, reconstituted in binary lipid bilayers composed of two phospholipids, DLPC and DSPC, with different hydrophobic acyl chain lengths. Exploiting the three facts that 1) BR has a specific and fixed hydrophobic length that presents a hydrophobic boundary conditions for the surronding lipids of the bilayer; 2) DLPC and DSPC, differing by six CH_2 units in their acyl chains, produce lipid bilayers with very different thicknesses; and 3) the hydrophobic thickness of the mixed lipid bilayers can be varied dramatically and systematically by changing temperature due to the chain melting phase equilibria; we are in the position of having an ideally suited model system to explore the importance of hydrophobic matching for lipid specificity and selectivity.

Altogether, comparison of theoretical and experimental lipid distributions provides a self-consistent view of the distribution of DLPC and DSPC around bacteriorhodopsin. At low and moderate temperatures, i.e., in the region of the phase diagram where DSPC is still in the gel state and DLPC is in the gel or fluid states, BR is clearly associated with the short-chain lipid. At high temperatures, when all of the lipids are in the fluid state, BR is preferentially associated with the long-chain lipid. In all cases, the condition of hydrophobic matching is satisfied. In this way, BR performs a kind of molecular sorting of the lipids in its neighborhood. The sorting may be seen as a type of physically controlled specificity in which no particular chemical forces are involved. There is no binding, and the special sorted lipid environment is a statistical entity of considerable dynamics. The extent of the associated lipid concentration profiles therefore strongly depends on thermodynamic conditions, i.e., the position in the phase diagram. Close to phase transitions and phase boundaries, the coherence length of the profiles can be very long. For other lipid mixtures, which have special critical mixing points, the possibility exists that the sorting may extend over macroscopic distances because of wetting.

A particularly striking finding of the present work is the indication that BR may display a tendency to position itself in the interfaces between gel and fluid lipid domains (cf. Fig. 10). The possibility of such an interfacial adsorption phenomenon was recently hypothesized to apply to BR in equimolar DMPC/DSPC mixtures, based on the way BR changed the gel-phase domain topology, as observed via measurements of the diffusional characteristics of fluorescent-labeled lipid analogs (Schram and Thompson, 1997). It is likely that the localization and accumulation of proteins in the interfaces of a lipid bilayer with domains will promote particularly strong direct protein-protein interactions and hence provide a vehicle for protein associations. It may be argued that the general validity of these results for the organization of biological membranes may be limited by the fact that gel domains are probably scarce or even unlikely under physiological conditions. However, it must be considered that in real biological membranes there is a large distribution of lipids varying in acyl chain lengths and that, for a given transmembrane protein, the various constitutive α-helices can vary in length and tilting angle with respect to the bilayer normal. Therefore, the above concept of lipid

sorting and preference of the protein for fluid-gel interfaces may be generalized by postulating that the protein is surrounded by more than one lipid species because each of its α-helices may select the type of lipid molecule whose acyl chains best match the actual helix length and tilting angle.

The function of BR is believed not to be associated with any conformational changes that alter the hydrophobic length of the membrane domain. However, this may be the case for other proteins, whose function therefore can be controlled by the lipid bilayer structure near the protein. Rhodopsin is an example of such an integral membrane protein, whose meta I to meta II transition, which is related to the visual process in the retina, recently has been shown to be influenced by the hydrophobic matching at the interface (Brown, 1994). It would obviously be of interest to extend the experimental techniques advanced in this paper to model membranes with rhodopsin to systematically explore the details of this triggering mechanism. Furthermore, it would be of interest to investigate whether structured concentration profiles around the protein might facilitate a medium-range lipid-mediated indirect protein-protein attraction that could have influence on the state of protein segregation and/or aggregation, which would be of biological relevance for those proteins whose biological activity depends on their aggregational state (Kaprelyants, 1988; Andersen, 1989).

It is likely that the molecular sorting mechanism described in the present paper in the case of bacteriorhodopsin is operative for a large class of integral membrane proteins. An example is the hydrophobic pulmonary surfactant proteins SP-C and SP-B, which were recently (Horowitz, 1995) shown by fluorescence energy transfer experiments to be associated with different palmitoyl lipids according to the hydrophobic matching principle. It is also likely that the molecular sorting mechanism and its overall effect on the organization of lipid-protein assemblies provides membranes with a general and effective means of compartmentalization by exploiting the slow reorganization dynamics of binary lipid mixtures (Jørgensen et al., 1996; Mouritsen et al., 1996; Schram and Thompson, 1997).

A further perspective of the present work is related to the general mechanism of drug action on membranes. Recent theoretical studies have suggested that certain drugs tend to accumulate along the dynamic interfaces between the fluid and the gel domains formed in the transition region of lipid bilayers (Jørgensen et al., 1991). Experimental work on the effects of general and local anesthetics on the acetylcholine receptor (Arias et al., 1990; Fraser et al., 1990) have further indicated that the drug changes the lipid-protein interfacial region. Hence it would be of interest, in light of the results presented in the present paper, to investigate whether part of the drug action is related to changes in the efficiency of protein-molecular sorting of lipids at the protein-lipid interface.

Tom E. Thompson is thanked for providing us with a preprint of his work on bacteriorhodopsin in binary lipid bilayers.

This work was supported by the Danish Natural Science Research Council, the Danish Technical Research Council, and the CNRS. OGM is a Fellow of the Canadian Institute for Advanced Research.

REFERENCES

Andersen, A. S. 1989. Reception and transmission. *Nature.* 337:12.

Arias, H. R., M. B. Sankaram, D. Marsh, and F. J. Barrantes. 1990. Effect of local anaesthetics on steroid-nicotinic acetylcholine receptor interactions in native membranes of *Torpedo marmorata* electric organ. *Biochim. Biophys. Acta.* 1027:287–294.

Bergelson, L. O., K. Gawrisch, J. A. Feretti, and R. Blumenthal, editors. 1995. Special issue on domain organization in biological membranes. *Mol. Membr. Biol.* 12:1–162.

Bloom, M., E. Evans, and O. G. Mouritsen. 1991. Physical properties of the fluid-bilayer component of cell membranes: a perspective. *Q. Rev. Biophys.* 24:293–397.

Brown, M. F. 1994. Modulation of rhodopsin function by properties of the membrane bilayer. *Chem. Phys. Lipids.* 73:159–180.

Brumm, T., K. Jørgensen, O. G. Mouritsen, and T. M. Bayerl. 1996. The effect of increasing membrane curvature on the phase transition and mixing behavior of a DMPC-DSPC lipid mixture as studied by Fourier transform infrared spectroscopy and differential scanning calorimetry. *Biophys. J.* 70:1373–1379.

Caffrey, M., and G. W. Feigenson. 1981. Fluorescence quencing in model membranes. 3. Relationship between calcium adenosinetriphosphate enzyme activity of the protein for phosphatidylcholines with different acyl chain characteristics. *Biochemistry.* 20:1949–1961.

Cornea, R. L., and D. D. Thomas. 1994. Effects of membrane thickness on the molecular dynamics and enzymatic activity of reconstituted Ca-ATPase. *Biochemistry.* 33:2912–2920.

Devaux, P. F., and M. Seigneuret. 1985. Specificity of lipid-protein interactions as determined by spectroscopic techniques. *Biochim. Biophys. Acta.* 822:63–125.

Eaton, B. R., and E. A. Dennis. 1976. Analysis of phospholipase C (*Bacillus cereus*) action toward mixed micelles of phospholipid and surfactant. *Arch. Biochem. Biophys.* 176:604–609.

Edidin, M. 1990. Molecular associations and lipid domains. *Curr. Top. Membr. Transp.* 36:81–96.

Fraser, D. M., S. R. W. Louro, L. I. Horváth, K. W. Miller, and A. Watts. 1990. A study of the effect of general anaestetics on lipid-protein interactions in acetylcholine receptors enriched membranes from *Torpedo nobiliana* using netroxide spin labels. *Biochemistry.* 29: 2664–2669.

Glaser, M. 1992. Characterization and formation of lipid domains in vesicles and erythrocyte membranes. *Comments Mol. Cell. Biophys.* 8:37–51.

Grainger, D. W., A. Reichert, H. Ringsdorf, and C. Salesse. 1989. An enzyme caught in action: direct imaging of hydrolytic function and domain formation of phospholipase A_2 in phosphatidylcholine monolayers. *FEBS Lett.* 252:73–82.

Gil, T., and L. Mikheev. 1995. Curvature controlled wetting in two dimensions. *Phys. Rev. E.* 52:772–780.

Hasselbacher, C. A., L. Terry, and T. G. Dewey. 1984. Resonance energy transfert as a monitor of membrane protein domain segregation: application to the aggregation of bacteriorhodopsin reconstituted into phospholipid vesicles. *Biochemistry.* 23:6445–6452.

Henderson, R., J. M. Baldwin, T. A. Ceska, F. Zemlin, E. Beckman, and K. H. Downing. 1990. Model of the structure of bacteriorhodopsin based on high-resolution electron cryo-microscopy. *J. Mol. Biol.* 213: 899–929.

Henderson, R., and P. N. T. Unwin. 1975. Three-dimensional model of purple membrane obtained by electron microscopy. *Nature.* 257:28–32.

Hønger, T., K. Jørgensen, R. L. Biltonen, and O. G. Mouritsen. 1996. Systematic relationship between phospholiphase A_2 activity and dynamic lipid bilayer microheterogeneity. *Biochemistry.* 35:9003–9006.

Horowitz, A. D. 1995. Exclusion of SP-C, but not SP-B, by gel phase palmitoyl lipids. *Chem. Phys. Lipids.* 76:27–39.

In't Veld, G., A. J. M. Driessen, J. A. F. Op den Kamp, and W. N. Konings. 1991. Hydrophobic membrane thickness and lipid-protein interactions of

the leucine transport system of *Lactococcus lactis*. *Biochim. Biophys. Acta.* 1065:203–212.

Ipsen, J. H., K. Jørgensen, and O. G. Mouritsen. 1990. Density fluctuations in saturated phospholipids increase as the acyl-chain length decreases. *Biophys. J.* 58:1099–1107.

Israelachvili, J. 1992. Intermolecular and Surface Forces. Academic Press, London.

Johannsson, A., C. A. Keithley, G. A. Smith, C. D. Richards, T. R. Hesketh, and J. C. Metcalfe. 1981a. The effect of bilayer thickness and *n*-alkanes on the activity of the (Ca^{2+}-Mg^{2+})-dependent ATPase of sarcoplasmic reticulum. *J. Biol. Chem.* 256:1643–1650.

Johannsson, A., G. A. Smith, and J. C. Metcalfe. 1981b. The effect of bilayer thickness on the activity of (Na^+-K^+)-ATPase. *Biochim. Biophys. Acta.* 641:416–421.

Jørgensen, K., J. I. Ipsen, O. G. Mouritsen, D. Bennett, and M. J. Zuckermann. 1991. The effects of density fluctuations on the partitioning of foreign molecules into lipid bilayers: application to anesthetics and insecticides. *Biochim. Biophys. Acta.* 1067:241–253.

Jørgensen, K., A. Klinger, M. Braiman, and R. L. Biltonen. 1996. Slow nonequilibrium dynamical rearrangement of the lateral structure of a lipid membrane. *J. Phys. Chem.* 100:2766–2769.

Jørgensen, K., and O. G. Mouritsen. 1995. Phase separation dynamics and lateral organization of two-component lipid membranes. *Biophys. J.* 95:942–954.

Jørgensen, K., M. M. Sperotto, O. G. Mouritsen, J. H. Ipsen, and M. J. Zuckermann. 1993. Phase equilibria and local structure in binary lipid bilayer. *Biochim. Biophys. Acta.* 1152:135–145.

Kaprelyants, A. S. 1988. Dynamic spatial distribution of proteins in the cell. *Trends Biochem. Sci.* 13:43–46.

Kechuan, T., D. J. Tobias, J. K. Blasie, and M. L. Klein. 1996. Molecular dynamics investigation of the structure of a fully hydrated gel-phase dipalmitoylphosphatidylcholine bilayer. *Biophys. J.* 70:595–608.

Kinnunen, P. K. J. 1991. On the principle of functional ordering in biological membranes. *Chem. Phys. Lipids.* 57:375–399.

Knoll, W., K. Ibel, and E. Sackmann. 1981. Small-angle neutron scattering study of lipid phase diagrams by the contrast variation method. *Biochemistry.* 20:6379–6383.

Knoll, W., G. Schmidt, and E. Sackmann. 1983. Critical demixing in fluid bilayers of phospholipid mixtures. A neutron diffraction study. *J. Chem. Phys.* 79:3439–3442.

Kusumi, A., and J. S. Hyde. 1982. Spin-label saturation-transfer electron spin resonance detection of transient association of rhodopsin in reconstituted membranes. *Biochemistry.* 21:5978–5983.

Le Bris, M. T., J. Mugnier, J. Bourson, and B. Valeur. 1984. Spectral properties of a new fluorescent dye emitting in the red: a benzoxazinone derivative. *Chem. Phys. Lett.* 106:124–127.

Lehtonen, J. Y. A., J. M. Holopainen, and P. K. J. Kinnunen. 1996. Evidence for fluid-fluid immiscibility of phospholipids in large unilamellar vesicles caused by hydrophobic mismatch. *Biophys. J.* 70: 1753–1760.

Lehtonen, J. Y. A., and P. K. J. Kinnunen. 1995. Phospholipase A_2 as a mechanosensor. *Biophys. J.* 68:1888–1894.

Lipowsky, R., and E. Sackmann, editors. 1995. Handbook of Biological Physics, Vol. 1. Elsevier Science B.V., Amsterdam.

Mabrey, S., and J. M. Sturtevant. 1976. Investigation of phase transitions of lipids and lipid mixtures by high sensitivity differential scanning calorimetry. *Proc. Natl. Acad. Sci. USA.* 76:3862–3866.

Mazères, S., V. Schram, J.-F. Tocanne, and A. Lopez. 1996. 7-Nitrobenz-2-oxa-1,3-diazole-4-yl-labeled phospholipids in lipid membranes: differences in fluorescence behaviour. *Biophys. J.* 71:327–335.

Mertz, K. M., Jr., and B. Roux, editors. 1996. Biological Membranes. A Molecular Perspective from Computation to Experiment. Birkhäuser, Boston.

Montecucco, C., G. A. Smith, F. Dabbeni-Sala, A. Johannsson, Y. M. Galante, and R. Bisson. 1982. Bilayer thickness and ezymatic activity in the mitochondrial cytochrome *c* oxidase and ATPase complex. *FEBS Lett.* 144:145–148.

Monti, J. A., S. T. Christian, and W. A. Shaw. 1978. Synthesis and properties of a highly fluorescent derivative of phosphatidylethanolamine. *J. Lipid Res.* 19:222–228.

Mouritsen, O. G. 1990. Computer simulation of cooperative phenomena in lipid membranes. *In* Molecular Description of Biological Membrane Components by Computer Aided Conformational Analysis. R. Brasseur, editor. CRC Press, Boca Raton, FL. 3–83.

Mouritsen, O. G., and R. L. Biltonen. 1993. Protein-lipid interactions and membrane heterogeneity. *In* Protein-Lipid Interactions (A. Watts, editor). Elsevier Science, Amsterdam. 1–39.

Mouritsen, O. G., and M. Bloom. 1984. Mattress model of lipid-protein interactions in membranes. *Biophys. J.* 46:141–153.

Mouritsen, O. G., and M. Bloom. 1993. Models of lipid-protein interactions in membranes. *Annu. Rev. Biophys. Biomol. Struct.* 22:145–171.

Mouritsen, O. G., B. Dammann, H. C. Fogedby, J. H. Ipsen, C. Jeppesen, K. Jørgensen, J. Risbo, M. C. Sabra, M. M. Sperotto, and M. J. Zuckermann. 1995. The computer as a laboratory for the physical chemistry of membranes. *Biophys. Chem.* 55:55–68.

Mouritsen, O. G., and K. Jørgensen. 1994. Dynamical order and disorder in lipid bilayers. *Chem. Phys. Lipids.* 73:3–25.

Mouritsen, O. G., and M. M. Sperotto. 1992. Thermodynamics of lipid-protein interactions in lipid membranes: the hydrophobic matching condition. *In* Thermodynamics of Cell Surface Receptors. M. Jackson, editor. CRC Press, Boca Raton, FL. 127–181.

Mouritsen, O. G., M. M. Sperotto, J. Risbo, Z. Zhang, and M. J. Zuckermann. 1996. Computational approach to lipid-protein interactions in membranes. *Adv. Comp. Biol.* 2:15–64.

Muderhwa, J. M., and H. L. Brockman. 1992. Lateral lipid distribution is a major regulator of lipase activity. *J. Biol. Chem.* 267:24184–24192.

Mustonen, P., J. A. Virtanen, P. Somerharju, and P. K. J. Kinnunen. 1987. Binding of cytochrome *c* to liposomes as revealed by the quenching of fluorescence from pyrene-labeled phospholipids. *Biochemistry.* 26: 2991–2997.

Nagle, J. F. 1993. Area/lipid of bilayer from NMR. *Biophys. J.* 64: 1476–1481.

Oesterhelt, D., and W. Stoeckenius. 1974. Isolation of the cell membrane of halobacterium halobium and its fractionation into red and purple membrane. *Methods Enzymol.* 31:667–678.

Pedersen, S., K. Jørgensen, T. Bækmark, and O. G. Mouritsen. 1996. Inirect evidence for lipid-domain formation in the transition region of phospholipid bilayers by two-probe fluorescence energy transfer. *Biophys. J.* 71:554–560.

Peschke, J, J. Riegler, and H. Möhwald. 1987. Quantitative analysis of membrane distortions introduced by mismatch of protein and lipid hydrophobic thickness. *Eur. Biophys. J.* 14:385–391.

Peterson, G. L. 1977. A simplification of the protein assay method of Lowry et al. which is more generally applicable. *Anal. Biochem.* 83: 346–356.

Piknová, B., E. Pérochon, and J.-F. Tocanne. 1993. Hydrophobic mismatch and long-range protein/lipid interactions in bacteriorhodopsin/phosphatidylcholine vesicles. *Eur. J. Biochem.* 218:385–396.

Pink, D. A., J. G. Green, and D. Chapman. 1980. Raman scattering in bilayers of saturated phosphatidylcholines. Experiment and theory. *Biochemistry.* 19:349–356.

Rehorek, M., N. A. Dencher, and M. P. Heyn. 1985. Long-range lipid-protein interactions. Evidence for time-resolved fluorescence depolarization and energy-transfer experiments with bacteriorhodopsin-dimyristoylphosphatidylcholine vesicles. *Biochemistry.* 24:5980–5988.

Rehorek, M., and M. P. Heyn. 1979. Binding of all-trans-retinal to the purple membrane. Evidence for cooperativity and determination of the extinction coefficient. *Biochemistry.* 18:4977–4983.

Rigaud, J. L., B. Pitard, and D. Levy. 1995. Reconstitution of membrane proteins into liposomes: application to energy transducing membrane proteins. *Biochim. Biophys. Acta.* 1231:223–246.

Sackmann, E. 1984. Physical basis of trigger processes and membrane structures. *In* Biological Membranes, Vol. 5. Academic Press. London. 105–143.

Sankaram, M. B., D. Marsh, and T. E. Thompson. 1992. Determination of fluid and gel domain sizes in two-component, two-phase lipid bilayers. *Biophys. J.* 63:340–349.

Sankaram, M. B., and T. E. Thompson. 1992. Deuterium magnetic resonance study of phase equilibria and membrane thickness in binary phospholipid mixed bilayers. *Biochemistry.* 31:8258–8268.

Schram, V., and T. E. Thompson. 1997. Influence of the intrinsic membrane protein bacteriorhodopsin on the gel phase domain topology in two-component phase-separated bilayer. *Biophys. J.* 72:2217–2225.

Schram, V., J. F. Tocanne, and A. Lopez. 1994. Influence of obstacles on lipid lateral diffusion: computer simulation of FRAP experiments and application to proteoliposomes and biomembranes. *Eur. Biophys. J.* 23:337–348.

Sperotto, M. M., and O. G. Mouritsen. 1991a. Mean-field and Monte Carlo simulation studies of the lateral distribution of proteins in membranes. *Eur. Biophys. J.* 19:157–168.

Sperotto, M. M., and O. G. Mouritsen. 1991b. Monte Carlo simulation studies of lipid order parameter profiles near integral membrane proteins. *Biophys. J.* 59:261–270.

Sperotto, M. M., and O. G. Mouritsen. 1993. Lipid enrichment and selectivity of integral membrane proteins in two component lipid bilayers. *Eur. Biophys. J.* 22:323–328.

Sternberg, B., P. Gale, and A. Watts. 1989. The effect of tempearture and protein content on the dispersive properties of bacteriorhodopsin from *H. halobium* in reconstituted DMPC complexes free of endogenous purple membrane lipids: a freeze-fracture electron microscopy study. *Biochim. Biophys. Acta.* 980:117–126.

Tocanne, J. F. 1992. Detection of lipid domains in biological membranes. *Comm. Mol. Cell. Biophys.* 8:53–72.

Tocanne, J. F., L. Cézanne, A. Lopez, B. Piknova, V. Schram, J. F. Tournier, and M. Welby. 1994. Lipid domains and lipid/protein interactions in biological membranes. *Chem. Phys. Lipids.* 73:139–158.

Werner, T. C., and R. M. Hoffman. 1973. Relation between an excited state geometry change and the solvent dependence of 9-methyl anthroate fluorescence. *J. Phys. Chem.* 77:1611–1615.

Yguerabide, J. 1994. Theory for establishing proximity relations in biological membranes by excitation energy transfer measurements. *Biophys. J.* 66:683–693.